ECS Journal of Solid State Science and Technology, **6** (12) P839-P844 (2017)
2162-8769/2017/6(12)/P839/6/$37.00 © The Electrochemical Society

Effects of Oxygen, Nitrogen and Fluorine on the Crystallinity of Tungsten by Hot-Wire Assisted ALD

Mengdi Yang, [z] **Antonius A. I. Aarnink, Rob A. M. Wolters, Jurriaan Schmitz,** **and Alexey Y. Kovalgin**

MESA+ Institute for Nanotechnology, University of Twente, 7500 AE Enschede, The Netherlands

A heated tungsten filament (wire) is well known to generate atomic hydrogen (at-H) by catalytically cracking molecular hydrogen (H_2) upon contact. This mechanism is employed in our work on hot-wire (HW) assisted atomic layer deposition (HWALD), a novel energy-enhancement technique. HWALD has been successfully utilized to deposit tungsten (W) films using alternating pulses of WF_6 and at-H. Depending on the conditions, either low-resistivity α- or higher-resistivity β-crystalline phases of W can be obtained. This work aims to clarify (i) which factors are decisive for the formed crystal phase and (ii) the role of the residual gases in the film growth mechanism. In this light, the effects of adding impurities (N_2O, O_2, NH_3 and H_2O) were investigated. Oxidizing species have a retarding effect on W growth but the process can be re-initiated after stopping their supply. In contrast, nitridizing species have a permanent inhibition effect. Further, the effects of WF_6 overdose were studied. The surplus of WF_6 appeared to be crucial for the process: in many cases this led to the formation of β-phase W instead of the α-phase, with a memory effect lasting for several deposition runs. Extra fluorine-containing species were thus identified as the likely cause of β-phase formation.
© 2017 The Electrochemical Society. [DOI: 10.1149/2.0241712jss] All rights reserved.

Manuscript submitted September 29, 2017; revised manuscript received November 27, 2017. Published December 6, 2017.

Atomic layer deposition (ALD) of metals has attracted considerable attention in recent years in view of its huge application potential in ultra-large-scale integrated circuit manufacturing. Plasma-enhanced ALD (PEALD) has been proposed as a technique which may be suitable to grow a number of metals, such as Pt,[1] Ru,[2,3] Co,[4] Al[5] and Cu.[6] However, plasma can cause damage to electron devices through the generation of ions and UV light.[7] In addition, a diversity of radicals, typically created in the plasma, activate numerous chemical side reactions besides the targeted one.[8,9] This makes the deposition kinetics and properties of the growing film hard to predict and control.

In our previous works[10–13] we have demonstrated an alternative and technically easier approach to replace the plasma in a PEALD process with a heated tungsten (W) wire (filament). It is well known that molecular hydrogen (H_2) can effectively decompose on a W filament heated to 1500–2000°C.[14–16] This so-called hot-wire (HW) assisted ALD (HWALD) is a novel energy-enhancement technique which has yet to be explored in detail and which has the potential to overcome the limitations of plasma-assisted processes. For example, damage caused by energetic ions and UV light does not occur as they cannot be formed by HW. Also, the diversity of the radicals can be reduced, making a HW source more monochromatic in terms of the reactive species formed.

In our recent work[10–13] HWALD was successfully utilized to deposit high-purity low-resistivity tungsten films using alternating pulses of WF_6 gas and atomic hydrogen (at-H), with the latter generated by the hot wire. The HWALD-W process appears to be inherently area selective, enabling the deposition of W films with little or no incubation time on W, Co and Si surfaces, and resulting in no deposition on TiN, Al_2O_3 and SiO_2 surfaces.[10–13] This greatly assists the so-called area-selective ALD (AS ALD), which is today a hot topic.

It is known that W can be formed in either low-resistivity α- or higher-resistivity β-crystalline phases.[17] With the former clearly being more attractive for applications in electronics. It is suggested that the β-phase can be formed either (i) via intermediate oxidation states or (ii) because of the presence of impurities.[18–22] The oxidation states (to be further reduced to pure W by e.g., at-H) can occur due to the presence of background oxidants (oxygen or water) in the system. (Note that even a base pressure of 10^{-7} mbar still gives an approximate flux of 0.1 monolayer/s to the substrate.) The other impurities can originate from the source gases, for example WF_6, so that the influence of fluorine-containing species needs to be considered as well.

In our deposition system we have been able to grow both phases of W by HWALD, depending on the actual reactor design and deposition conditions. However, factors leading to the preferential formation of one of the phases over the other are still to be determined. To clarify the occurrence of the β-phase, this work investigates the effects of adding oxidizing and nitridizing gases such as N_2O, O_2, NH_3 and H_2O, as well as an WF_6 overdose, on HWALD of W. In addition, the mechanism of this ALD process in terms of chemical reactions on the surface remains doubtful. On the one hand, after each pulse WF_6 can dissociatively chemisorb on the as-grown metallic surface, leaving fluorine termination, to be removed by the subsequent at-H pulse. On the other hand, chemisorption can occur via the mentioned intermediate oxidation states, resulting in the reaction of WF_6 with, for example, OH-groups on the surface. As these groups merely originate from the base-pressure gases, their surface concentration cannot be high and should thus limit the deposition. The controllable addition of small amounts of oxidants to the gas phase would then increase the growth rate. Accordingly, the experiments reported in this paper aim to clarify the deposition mechanism as well.

Experimental

Deposition of HWALD tungsten films.—In our experiments, 100 nm silicon oxide (SiO_2) was thermally grown on 4-inch silicon p-type Si (100) wafers as a substrate for W deposition. Prior to deposition, the wafers were cleaned in fuming (99%) HNO_3 and boiling 69% HNO_3 to remove organic and metallic contamination, respectively. Then the substrates were immersed in 0.3% HF solution for 3 min. To circumvent the very slow nucleation of tungsten on SiO_2,[23] a W seed layer of average thickness 2 to 5 nm was pre-formed on SiO_2 at a substrate temperature of 325°C. It was formed by (i) growing a few-nm-thick amorphous Si (a-Si) layer using trisilane gas and (ii) subsequently exposing the a-Si to WF_6 gas, producing a solid W film together with volatile silicon fluorides. The details regarding the formation of this seed layer have been elaborated elsewhere.[11,12]

The W films were grown on this seed layer using WF_6 and at-H by the HWALD process developed in our previous work.[13] Importantly, during all the experiments, only one precursor (H_2) passed the remotely mounted hot wire, whereas the other gases were introduced through lateral gas inlets surrounding the wafer. The standard HWALD process conditions were fixed at a substrate temperature of 275°C and a total pressure of 0.05 mbar. A single **ALD cycle** consisted of an at-H (50 sccm of H_2) pulse of 7 s duration, a post-at-H purge of 7 s and a WF_6 (3 sccm) pulse of 0.5 s followed by a post-WF_6 purge of 7 s. The hot-wire temperature was kept at 1750°C.

All deposition experiments were carried out in a custom-built **hot-wall** reactor,[10,24–26] equipped with an in situ Woollam M-2000 spectroscopic ellipsometer (SE) operating in the wavelength range 245–1688 nm. The SE enabled in situ monitoring of the surface processes

[z]E-mail: m.yang@utwente.nl

Downloaded on 2018-01-22 to IP 130.89.46.109 address. Redistribution subject to ECS terms of use (see ecsdl.org/site/terms_use) unless CC License in place (see abstract).

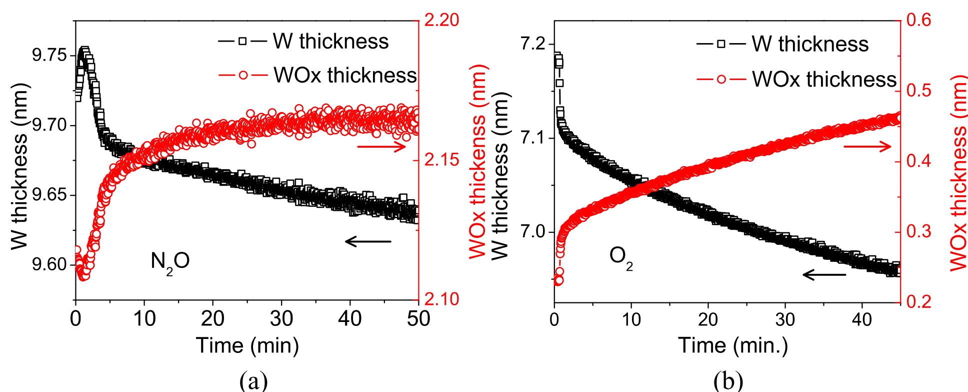

Figure 1. Oxidation measured by in situ Spectroscopic Ellipsometer (SE) while exposing the pre-grown HWALD W films to a continuous flow (3 sccm) of N_2O (a) or O_2 (b) at 275°C and a pressure of 0.05 mbar. The hot wire was turned off in these experiments.

in real time. One should bear in mind that all sub-nanometer (sub-monolayer) thickness variations depicted in Figure 2c, Figure 5 and Figure 7a indicate only a qualitative trend (i.e., increase, decrease or hardly any change) in thickness behavior and do not provide reliable quantitative information due to the sensitivity margins of the SE. The crystallinity of the grown W films was examined by X-ray diffraction (XRD) and their elemental composition was determined by X-ray photoelectron spectroscopy (XPS).

Methodology to study the influence of additional gases.—In this work we studied the influence of small amounts of N_2O, O_2, NH_3 and H_2O gases, as well as WF_6 overdose, on the growth rate per cycle (GPC), composition and crystallinity of HWALD W films. The films were first grown to a certain thickness (4–10 nm) at standard process conditions. Then, they were exposed to either a continuous flow or short pulses of a selected gas in the same reactor, keeping the gas pressure and temperature unchanged. It should be noted that 1 pulse of a selected gas was added after a number (1 or 3) of full HWALD cycles.

The pulse time was varied between 0.1–2 s for N_2O and O_2, maintaining a purge time of 7 s to remove these gases prior to every subsequent HWALD cycle. For water vapor (H_2O), the pulse and purge times were 5 and 10 s, respectively. The dose of H_2O was determined by its vapor pressure (approximately 60 mbar) in the bottle and the pulse time. NH_3, as a source of nitridizing species, was only introduced at a constant flow of 20 sccm to investigate possible differences between the oxidation and nitridation effects. The WF_6 overdose was achieved by (i) increasing the WF_6 flow from 3 to 10 sccm, (ii) prolonging the WF_6 pulse time from 0.1 to 3 s and (iii) performing the HWALD process for more than 2 hours with 0.5-s-long WF_6 pulses.

Results and Discussion

Influence of N_2O and O_2 on the HWALD W process.—The results of the real-time monitoring of oxidation by a continuous flow of either N_2O or O_2 are shown in Figure 1. The optical functions of HWALD W were successfully parameterized using a Drude-Lorentz description consisting of a Drude term and two Lorentz oscillators.[27] The tungsten oxide (WO_x) was modelled by a Tauc-Lorentz formulation.[28] The fitted thickness of the HWALD W was verified by high-resolution scanning electron microscopy (HRSEM), as demonstrated in earlier work.[11] However, the thickness of the tungsten oxide (WO_x) films could not be confirmed by ex situ techniques due to its small value. The WO_x thicknesses reported in this article can therefore only be used for qualitative analysis. Nevertheless, the change of oxide thickness in Figure 1 is fully coherent with that of HWALD W, revealing simultaneous oxide growth (by both N_2O and O_2) and reduction of the W film thickness. Assuming the thickness values to be correct, one can conclude that W oxidizes faster in O_2 (Figure 1b) than in N_2O (Figure 1a), probably due to a higher reactivity and/or diffusivity of O_2.

In Figure 2, a selected oxidant was briefly introduced after every three full HWALD cycles. It can be observed that the GPC was suppressed by these additional pulses and diminished further with increasing pulse duration. The negative GPC seen in Figure 2b for the O_2 pulses longer than 0.5 s can be can be understood as the effect of film oxidation which reduces the W film thickness. Exposure to N_2O

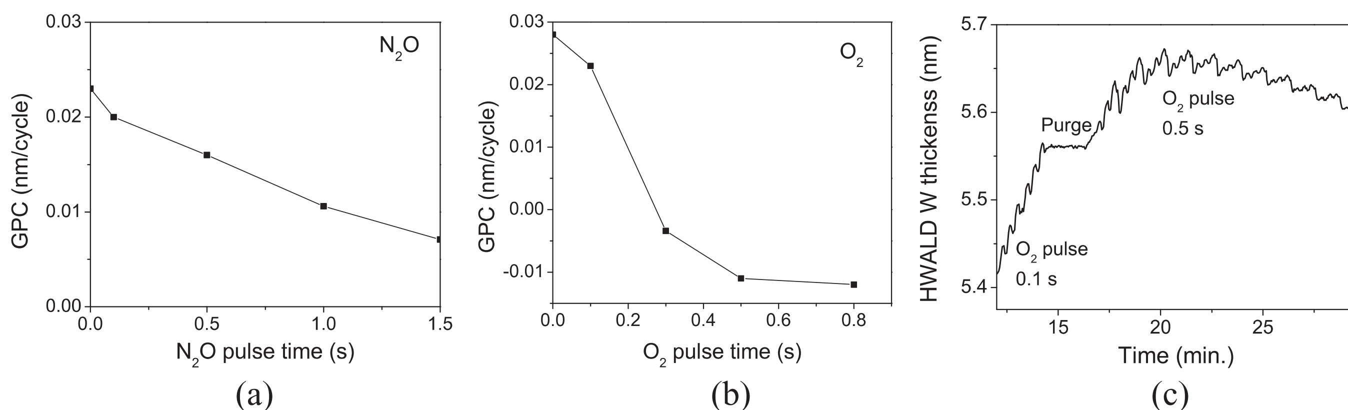

Figure 2. In situ SE measurements performed at 275°C and 0.05 mbar. A decrease of GPC of HWALD W films during additional N_2O (a) and O_2 (b) pulses after each 3 standard HWALD cycles with a 7 s Ar purge in between. The negative growth rate observed for the longer O_2 pulses corresponds to dominating oxidation. (c) Transition from growth to dominating oxidation when O_2 pulse was increased from 0.1 s to 0.5 s.

Downloaded on 2018-01-22 to IP 130.89.46.109 address. Redistribution subject to ECS terms of use (see ecsdl.org/site/terms_use) unless CC License in place (see abstract).

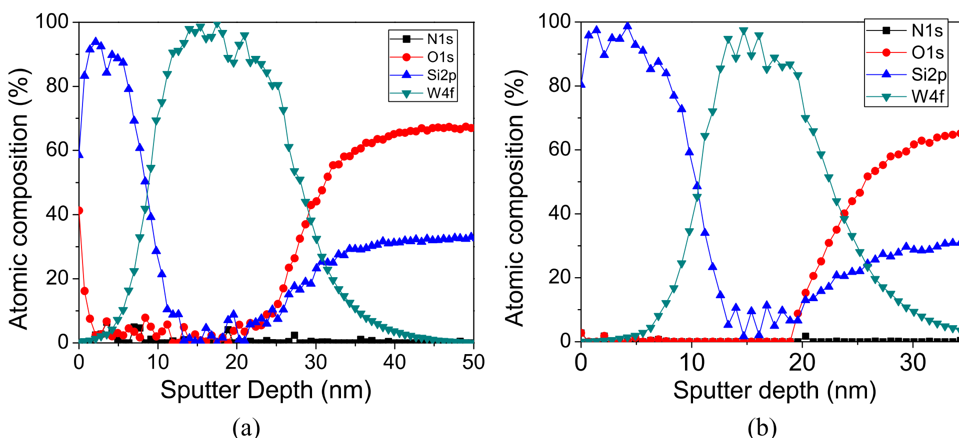

Figure 3. XPS depth profiles of 15-nm thick HWALD W films grown at 275°C and 0.05 mbar with additional (a) O_2 and (b) N_2O pulses.

gas was less effective in reducing the GPC (Figure 2a), which is in agreement with the higher oxidation rate in O_2 compared to N_2O observed in Figure 1. Moreover, the transition from growth to reducing thickness due to oxidation can be clearly seen in Figure 2c, where the pulse time of the O_2 was increased from 0.1 s to 0.5 s. The steps represent individual HWALD cycles. Apparently, an O_2 pulse of 0.1 s had little influence on the GPC. However, oxidation started to take over the deposition when the O_2 pulse time was increased to 0.5 s, resulting in a gradual decrease of the total W thickness after approx. 23 min (Figure 2c). For N_2O gas, the film growth still dominated over oxidation for a pulse time of 1.5 s. Once again, one can see a smaller effect of N_2O compared to O_2.

Further, 15-nm thick HWALD W films were deposited with additional pulses (0.1 s) of either N_2O or O_2, as described above. The films were capped with a 10-nm a-Si to prevent their oxidation upon exposure to air. Figure 3 shows XPS depth profiles depicting the elemental composition of these two films. In spite of their periodic exposure to oxidants, a very low concentration of oxygen is present throughout the layer below the a-Si cap, indicating an effective reduction of the tungsten oxide by at-H. The resistivity values, measured by a four-point probe method, varied between 20 and 28 μΩ•cm, which is comparable with the values obtained for a HWALD W deposited without additional O_2 pulses (i.e., about 15 μΩ•cm[13]). Further, the film grown with additional pulses of N_2O (Figure 3b) hardly contains any nitrogen.

The low resistivity of HWALD films deposited with O_2 pulses implies the presence of α-phase W, as the resistivity of β-phase W is normally above 100 μΩ · cm.[17] To verify the crystallinity, an XRD analysis was carried out and the XRD scan is presented in Figure 4. It should be noted that only crystals with crystal planes oriented parallel to the substrate can be observed by a θ–2θ scan. The four distinguishable peaks, located at 40.2° ((110) plane), 58.2° ((200) plane), 73.2° ((211) plane) and 87.1° ((220) plane), are unique for α-phase W.[17] The strongest peak at around 69° corresponds to the Si (100) substrate. No peaks associated with β-phase W can be observed. It can be concluded that the HWALD W exists in α-phase form, even when exposed to oxidants during the process.

Influence of H_2O vapor on the HWALD W process.—As H_2O vapor is constantly present at the background level (i.e., 10^{-7} mbar), it might also influence the HWALD process. To investigate the effect of water vapor, an H_2O pulse of 5 s was inserted after each HWALD cycle, followed by an Ar purge of 10 s. The GPC was greatly inhibited by H_2O (Figure 5), decreasing from 0.018 to only 0.006 nm/cycle after as few as two H_2O pulses. The very slow growth rate after the water treatment made the preparation of samples thick enough for XPS or XRD practically impossible. Remarkably, the in situ SE monitoring of individual cycles (Figure 5) consistently revealed a thickness change of around 0.05 nm after the first H_2O pulse, quickly diminishing for

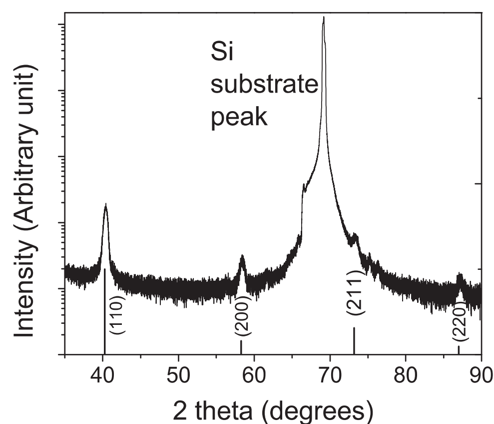

Figure 4. XRD pattern of the film presented in Figure 3 (a), showing α-phase W. The vertical straight lines indicate the known peaks of α-phase W.

each subsequent H_2O pulse. This step is much higher than the standard GPC (approx. 0.02 nm/cycle) without H_2O; it is possible that the first H_2O pulse enhances the growth rate. However, giving further pulses quickly suppresses the first-pulse effect. The decay of the GPC can be interpreted by blocking (occupation of) the surface sites by water; such adsorption processes often show an exponential dependence in time.

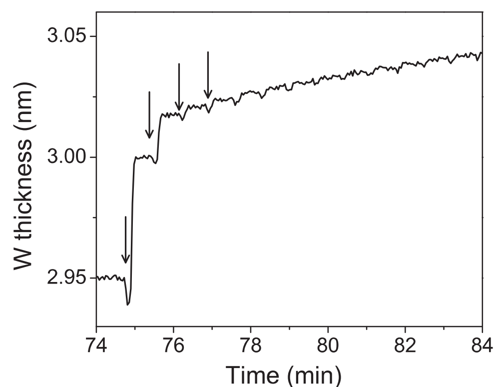

Figure 5. The effect of decreasing GPC due to additional H_2O-vapor pulses of 5 s (followed by a purge of 10 s) inserted after each standard HWALD cycle. The steps represent individual cycles visualized by SE. Arrows indicate each H_2O pulse.

Downloaded on 2018-01-22 to IP 130.89.46.109 address. Redistribution subject to ECS terms of use (see ecsdl.org/site/terms_use) unless CC License in place (see abstract).

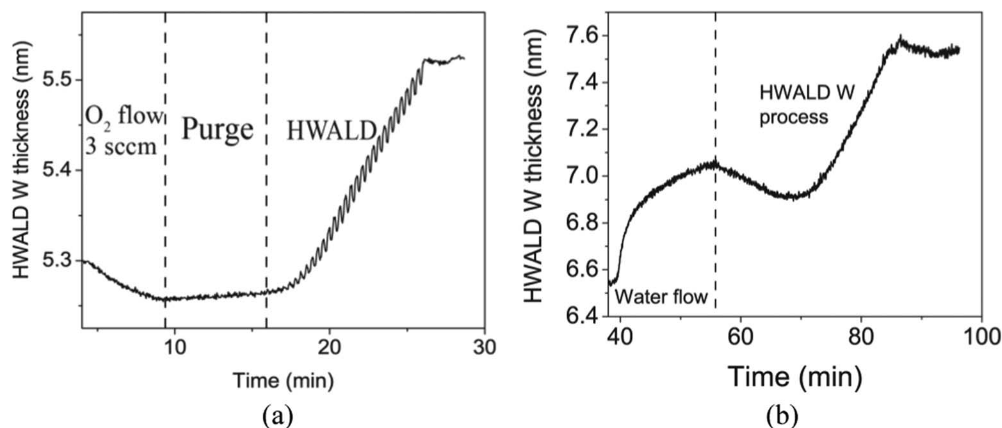

Figure 6. Recovery of the HWALD process after terminating the constant (a) oxygen flow and (b) H_2O flow. The processes are monitored in real time by in situ SE.

Growth recovery after oxidation and its termination by nitrogen-containing gases.—Our experiments demonstrated that an oxidized W surface can be reduced by at-H, recovering the film growth after a sufficient reduction time. Namely, after the exposure of a 10-nm-thick HWALD W film to air for 900 hours, a 20-min reduction in at-H at 275°C was sufficient to restart the HWALD process and to reach the standard GPC after 150 cycles. Figure 6a shows a quick GPC recovery after a 5-min exposure to 3 sccm of O_2. Remarkably, in this example, the GPC recovered to the original value after an incubation time of around 30 cycles, even without any additional at-H reduction. This implied that, during the incubation time, the oxides were effectively reduced by the at-H of the HWALD cycles. Similarly, in Figure 6b, it can be seen that the GPC could recover within approx. 40 HWALD cycles after the H_2O treatment. This also implies the reduction of surface oxides by the at-H.

It was additionally found that N_2O-exposure tends to inhibit or even stop the HWALD process, in contrast to an O_2 exposure. Namely, no growth was observed for at least 15 min after exposure to an N_2O flow of 3 sccm for 5 min, see Figure 7a, while the same flow rate and comparable time resulted in a successful recovery of the GPC in case of O_2 exposure, see Figure 6a. This difference suggested a crucial change to the surface, which could well have been caused by a nitrogen-containing species forming at the surface. To investigate this further, N_2O was replaced by NH_3. As shown in Figure 7b, after an exposure to NH_3 (20 sccm) for 10 min, HWALD cycling did not lead to W deposition for at least 20 min. This confirmed nitridation of the surface as preventing the HWALD W process. Not only did a tungsten nitride surface inhibit HWALD of W; we earlier found no measurable growth of W on TiN after 600 HWALD cycles.[13]

Clarifying the actual film-growth mechanism remains outside the scope of this work and it would require an extended study of the surface chemistry. We however speculate that WF_6 can dissociatively adsorb on a metallic (e.g., W and Co) surface, from which the fluorine termination is removed by the subsequent at-H pulse, forming gaseous HF and leaving the pure metallic surface. For an oxidized surface, W or Co oxides can still be reduced by at-H to pure metals.[29] In case of having non-reducible oxides such as SiO_2 and Al_2O_3, at least in the temperature range studied, existence of the oxide prohibits deposition of W[29] presumably by inhibiting the chemisorption of WF_6. We assume that similar holds for certain nitrides (e.g., TiN) and/or a nitridized W surface, as they are thermodynamically difficult to reduce back to metals. For example, our earlier studies with in-situ SE show no measurable reduction of TiN by at-H at low temperatures. However, the growth of W on such surfaces may still be enabled at a higher substrate temperature.

Influence of WF_6 overdose on the HWALD W process.—The experiments with oxygen- and nitrogen-containing gases did not clarify the original cause of β-phase formation. In our earlier experiments using a cold-wall reactor growth of β-phase W was always observed[11] and only when the processes were carried out in a hot-wall reactor was α-phase W successfully generated.[13] The wide range of experiments supported the assumption that fluorine remnants in the reactor, possibly adsorbing on the cold walls, play a role in β-phase formation.

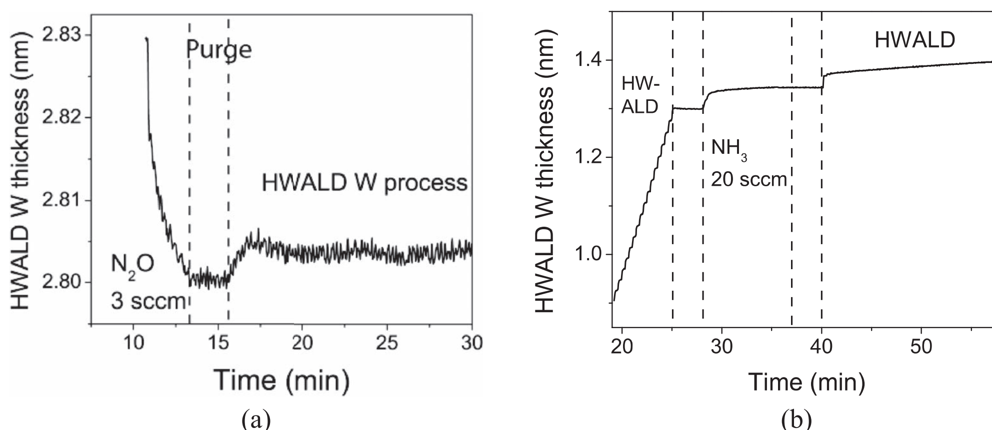

Figure 7. No recovery of the HWALD process after terminating the constant (a) N_2O flow of 3 sccm and (b) NH_3 flow of 20 sccm. The vertical dashed lines confine the Ar-purge regions in time. The processes are monitored in real time by in situ SE.

Downloaded on 2018-01-22 to IP 130.89.46.109 address. Redistribution subject to ECS terms of use (see ecsdl.org/site/terms_use) unless CC License in place (see abstract).

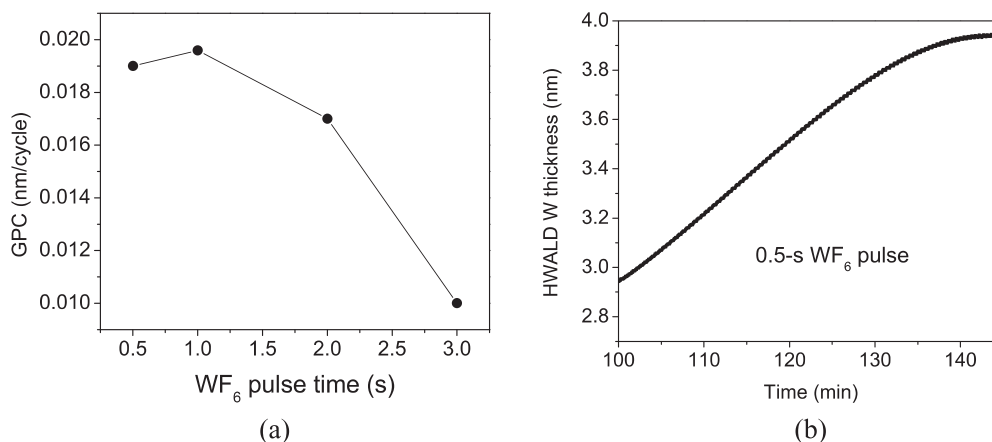

Figure 8. The influence of WF_6 overdose on the growth rate of HWALD W. (a) The decreasing GPC versus WF_6 pulse time for a WF_6 flow of 10 sccm indicates the etching effect.[12] The post-WF_6-purge time (with Ar) after each WF_6 pulse was set to 10 s. (b) Lowering GPC observed after more than 2 hours due to accumulation of fluorine compounds in the reactor for slightly longer (0.5 s compared to standard 0.2 s) WF_6 pulses. The processes are monitored by in situ SE.

To investigate this effect further in the hot-wall reactor, we increased the WF_6 pulse time and flow in the hot-wall ALD cycle, resulting in a long-term excess of fluorine-containing species (WF_x, F_2, atomic fluorine; which we will refer to fluorine compounds) in the reactor. As seen in Figure 8a, such WF_6 overdose resulted in a suppression of the growth rate. For a WF_6 flow rate of 10 sccm (note that 3 sccm corresponds to our standard condition), the GPC gradually decreased from 0.02 to 0.01 nm/cycle with increasing pulse time. This decrease in GPC was earlier attributed to film etching by fluorine compounds due to a coexistence of deposition and etching modes in the same process.[12] This was likely caused by the excess background pressure of the fluorine compounds.

We further decreased the WF_6 flow back to 3 sccm while keeping the WF_6 pulse time at 0.5 s, i.e., slightly longer compared to the standard 0.2 s. As seen in Figure 8b, performing the HWALD process with these prolonged pulses resulted in a noticeable lowering the GPC after more than 2 hours. This further confirmed the slow accumulation of the fluorine compounds in the reactor under non-optimized WF_6-exposure conditions.

All of the experiments carried out with excess-fluorine showed a decrease of the GPC. For large overdoses, the as-grown films exhibited a resistivity above 100 $\mu\Omega \cdot$ cm, pointing to the formation of β-phase W. This was further confirmed by the XRD spectra. A comparison of the XRD spectra for α- and β-phase W can be found in our previous work.[11]

According to our previous experience,[13] increasing the H_2/at-H dose did not cause any beta-phase formation. In this work we have shown that beta phase can readily be formed with a higher background pressure of fluorine-containing compounds. These background fluorine-containing species could comprise WF_6, HF, F_2 (or F), and a variety of WF_x ($x < 6$) sub-fluorides being generated due to the thermal dissociation of the background WF_6 upon the hot wire.[30] As mentioned before, beta-phase W was proposed to be formed if additional gaseous impurities were present during deposition.[18–22] It was also reported that the sub-fluorides could react with residual oxygen-containing gases to form volatile compounds.[31] All mentioned species could in principle lead to the beta-phase W. Unfortunately, it is difficult to determine the threshold background pressure of fluorine compounds which when exceeded results in the formation of β-phase W without a direct measurement of the gas phase composition. This remains outside the scope of this work, together with the precise identification of these compounds. Nevertheless, a surplus of fluorine compounds in the gas phase is likely to influence the film crystallinity even in the hot-wall reactor. With a sufficient WF_6 overdose, the background fluorine compounds could lead to the formation of β-phase W instead of the α-phase with a memory effect lasting for several deposition runs. Extra fluorine compounds present in the reactor are thus proposed as the potential root cause of β-phase W formation.

Conclusions

In this work, the effects of adding N_2O, O_2, NH_3 and H_2O gasses on HWALD of W have been investigated. The growth rate per cycle can be suppressed by additional N_2O, O_2 and H_2O pulses and decays with increasing the pulse duration. The as-grown films however exhibit a high purity α-phase W, indicating an efficient reduction of tungsten oxides by atomic H. Among these oxidants, water appears to have the strongest impact on the suppression of the growth rate. It is however possible to successfully restart the HWALD process (after a certain incubation time) and recover the original GPC after removing H_2O or O_2 from the deposition chamber. In contrast, additional NH_3 or N_2O pulses can entirely terminate the HWALD process, depending on the dose and/or exposure time. This termination is presumably caused by nitridation of the W surface. Finally, we investigated the influence of a temporary WF_6 overdose, which led to a long-term excess of fluorine compounds in the reactor. Increasing the WF_6 pulse time decreases the GPC due to the coexistence of film etching. With a sufficient WF_6 overdose, the as-grown films exhibit a resistivity above 100 $\mu\Omega \cdot$ cm. This indicates the formation of β-phase W, further confirmed by the XRD spectra. We conclude that the surplus of fluorine-containing species is likely to cause the formation of β-phase W.

Acknowledgments

We thank the NWO Domain Applied and Engineering Sciences (NWO-TTW) for the financial support of this project (12846).

ORCID

Mengdi Yang https://orcid.org/0000-0003-4983-7963
Jurriaan Schmitz https://orcid.org/0000-0002-9677-825X

References

1. D. Longrie, K. Devloo-Casier, D. Deduytsche, S. V. d. Berghe, K. Driesen, and C. Detavernier, *J. Solid State Sci. Technol.*, **1**, Q123 (2012).
2. O.-K. Kwon, S.-H. Kwon, H.-S. Park, and S.-W. Kang, *J. Electrochem. Soc.*, **151**, C753 (2004).
3. O.-K. Kwon, S.-H. Kwon, H.-S. Park, and S.-W. Kang, *Electrochem. Solid St. Lett.*, **7**, C46 (2004).
4. H. Kim, *Electrochem. Solid St. Lett.*, **9**, G323 (2006).
5. Y. J. Lee and S. W. Kang, *Electrochem. Solid St. Lett.*, **5**, C91 (2002).

Downloaded on 2018-01-22 to IP 130.89.46.109 address. Redistribution subject to ECS terms of use (see ecsdl.org/site/terms_use) unless CC License in place (see abstract).

6. J. Mao, E. Eisenbraun, V. Omarjee, A. Korolev, C. Lansalot, and C. Dussarrat, *ECS Trans.*, **33**, 125 (2010).
7. V. V. Afanas'ev, J. M. M. de Nijs, and P. Balk, *J. Appl. Phys.*, **78**, 6481 (1995).
8. M. J. Kushner, *J. Appl. Phys.*, **71**, 4173 (1992).
9. C. Mogab, A. Adams, and D. L. Flamm, *J. Appl. Phys.*, **49**, 3796 (1978).
10. A. Y. Kovalgin, M. Yang, S. Banerjee, R. O. Apaydin, A. A. Aarnink, S. Kinge, and R. A. M. Wolters, *Adv. Mater. Interfaces*, **4**, 1700058 (2017).
11. M. Yang, A. A. Aarnink, A. Y. Kovalgin, D. J. Gravesteijn, R. A. Wolters, and J. Schmitz, *J. Vac. Sci. Technol. A*, **34**, 01A129 (2016).
12. M. Yang, A. A. Aarnink, A. Y. Kovalgin, R. A. Wolters, and J. Schmitz, *Phys. Status Solidi A*, **212**, 1607 (2015).
13. M. Yang, A. A. I. Aarnink, J. Schmitz, and A. Y. Kovalgin, "Low-resistivity α-phase tungsten films grown by hot-wire assisted ALD in high-aspect-ration structures," *Thin Solid Films*, to be published.
14. I. Langmuir, *J. Am. Chem. Soc.*, **34**, 860 (1912).
15. I. Langmuir and G. M. J. Mackay, *J. Am. Chem. Soc.*, **36**, 1708 (1914).
16. I. Langmuir, *J. Am. Chem. Soc.*, **37**, 417 (1915).
17. E. Lassner and W. D. Schubert, *Tungsten: Properties, Chemistry, Technology of the Elements, Alloys, and Chemical Compounds*, Springer Science & Business Media, New York (1999).
18. D. P. Basile, C. L. Bauer, S. Mahajan, A. G. Milnes, T. N. Jackson, and J. DeGelormo, *Mater. Sci. Eng. B*, **10**, 171 (1991).
19. A. Bensaoula, J. C. Wolfe, A. Ignatiev, F. O. Fong, and T. S. Leung, *J. Vac. Sci. Technol. A*, **2**, 389 (1984).
20. M. J. O'Keefe and J. T. Grant, *J. Appl. Phys.*, **79**, 9134 (1996).
21. Y. Pauleau, P. Lami, A. Tissier, R. Pantel, and J. C. Oberlin, *Thin Solid Films*, **143**, 259 (1986).
22. J. H. Souk, J. F. O'Hanlon, and J. Angillelo, *J. Vac. Sci. Technol. A*, **3**, 2289 (1985).
23. J. E. J. Schmitz, *Chemical Vapor Deposition of Tungsten and Tungsten Silicides for VLSI/ULSI Applications*, p. 12, Noyes, Park Ridge NJ (1992).
24. S. Bystrova, A. Aarnink, J. Holleman, and R. Wolters, *J. Electrochem. Soc.*, **152**, G522 (2005).
25. H. Van Bui, A. Y. Kovalgin, A. A. I. Aarnink, and R. A. M. Wolters, *J. Solid State Sci. Technol.*, **2**, P149 (2013).
26. H. Van Bui, F. Grillo, and J. van Ommen, *Chem. Commun.*, **53**, 45 (2017).
27. F. Wooten, *Optical Properties of Solids*, p. 52, Academic Press, New York (1972).
28. J. Tauc, R. Grigorovici, and A. Vancu, *Phys. Status Solidi B*, **15**, 627 (1966).
29. M. Yang, A. A. I. Aarnink, J. Schmitz, and A. Y. Kovalgin, "Inherently area-selective hot-wire assisted atomic layer deposition of tungsten films," *Thin Solid Films*, to be published.
30. J. Creighton, *J. Vac. Sci. Technol. A*, **7**, 621 (1989).
31. T. D. Bestwick and G. S. Oehrlein, *J. of Appl. Phys.*, **66**, 5034 (1989).

Downloaded on 2018-01-22 to IP 130.89.46.109 address. Redistribution subject to ECS terms of use (see ecsdl.org/site/terms_use) unless CC License in place (see abstract).